PHYSOR-2006, ANS Topical Meeting on Reactor Physics
Organized and hosted by the Canadian Nuclear Society. Vancouver, BC, Canada. 2006 September 10-14

Sensitivity of MCNP5 Calculations for a Spherical Numerical Benchmark Problem to the Angular Scattering Distributions for Deuterium

Ken S. Kozier

Atomic Energy of Canada Limited, Chalk River Laboratories, Chalk River, ON, K0J 1J0 Canada

Abstract

This paper examines the sensitivity of MCNP5 k_{eff} results to various deuterium data files for a simple benchmark problem consisting of an 8.4-cm radius sphere of uranium surrounded by an annulus of deuterium at the nuclide number density corresponding to heavy water. This study was performed to help clarify why Δk_{eff} values of about 10 mk are obtained when different ENDF/B deuterium data files are used in simulations of critical experiments involving solutions of high-enrichment uranyl fluoride in heavy water, while simulations of low-leakage, heterogeneous critical lattices of natural-uranium fuel rods in heavy water show differences of <1 mk. The benchmark calculations were performed as a function of deuterium reflector thickness for several uranium compositions using deuterium ACE files derived from ENDF/B-VII.b1 (release beta1), ENDF/B-VI.4 and JENDL-3.3, which differ primarily in the energy/angle distributions for elastic scattering <3.2 MeV. Calculations were also performed using modified ACE files having equiprobable cosine bin values in the centre-of-mass reference frame in a progressive manner with increasing energy. It was found that the Δk_{eff} values increased with deuterium reflector thickness and uranium enrichment. The studies using modified ACE files indicate that most of the reactivity differences arise at energies <1 MeV; hence, this energy range should be given priority if new scattering distribution measurements are undertaken.

KEYWORDS: deuterium, MCNP5, angular scattering, numerical benchmark

1. Introduction

During post-release testing of the final release of version VI of the Evaluated Nuclear Data File (ENDF/B-VI.8), staff at the Los Alamos National Laboratory (LANL) discovered [1, 2] that the eigenvalues (k_{eff}) calculated for a series of heavy-water (D_2O) solution critical benchmark experiments had decreased by about 10 mk relative to results obtained using earlier versions of the ENDF/B-VI data library for deuterium (releases VI.0 to VI.4). The benchmark experiments in question involved two sets of High-enriched-uranium (HEU) Solution Thermal (HST) critical experiments (HST-004 and -020 [3]) that were performed at LANL in the early 1950s using simple, high-neutron-leakage (about 40%) arrangements of homogeneous solutions of uranyl fluoride in D_2O at various concentrations. HST-004 included six measurements with spheres reflected by D_2O while HST-020 involved five measurements with unreflected cylinders.

In contrast, only small reactivity differences (<1 mk) are observed [4] when similar substitutions of the deuterium nuclear data are made in MCNP5™[a] [5] (Monte Carlo N-Particle) simulations of critical measurements involving low-leakage (about 11% from the moderator surfaces), heterogeneous lattices of natural-uranium (NU) fuel rods immersed in D_2O moderator in the ZED-2 (Zero Energy Deuterium) research reactor at the Chalk River Laboratories. The objective of this work is to investigate the reasons for these different results by performing additional MCNP5 simulations using a very simple spherical numerical benchmark model.

2. Method

2.1 Benchmark Model

A very simple spherical MCNP5 numerical model was constructed to isolate and highlight some of the key factors giving rise to the different Δk_{eff} sensitivities of the HST and ZED-2 critical experiments to the deuterium nuclear data.

The benchmark model configuration was chosen to emphasize the reactivity impact of angular scattering from deuterium, specifically the reactivity enhancement due to backscattering from a deuterium neutron reflector. Moreover, for clarity, the model uses at most three nuclides: ^{235}U, ^{238}U and ^{2}H (=D). Accordingly, the model consisted of an 8.4-cm-radius sphere of uranium metal surrounded by a concentric spherical annulus of deuterium (at a nuclide number density of $6.60\text{x}10^{-2}$ atoms/barn·cm, corresponding to D_2O) of variable thickness (up to 100 cm) at room temperature (293.6 K). The calculated k_{eff} for the model is near critical (MCNP5 $k_{eff} = 0.998$) when the inner sphere is pure ^{235}U metal (nuclide number density = $4.82\text{x}10^{-2}$ atoms/barn·cm) with no deuterium reflector. For simplicity, the $S(\alpha,\beta)$ thermal scattering treatment for deuterium in D_2O was not used. Calculations were also performed for an NU-metal (^{235}U number density = $3.47\text{x}10^{-4}$ atoms/barn·cm; ^{238}U number density = $4.78\text{x}10^{-2}$ atoms/barn·cm) inner sphere and for pure ^{235}U and ^{238}U spheres at the aforementioned nuclide number densities corresponding to NU.

2.2 Nuclear Data Input

The MCNP5 calculations were performed using ACE (A Compact ENDF format) input files that were prepared elsewhere. The ^{235}U and ^{238}U ACE files were derived from ENDF/B-VII.b1 (release beta1). The deuterium ACE files tested correspond to: ENDF/B-VII.b1 (similar to VI.5 to VI.8), used as the reference; ENDF/B-VI.4 (similar to VI.0 to VI.4); and JENDL-3.3 [6].

The ENDF/B-VII.b1 deuterium data are based on a coupled-channels R-matrix analysis for the elastic scattering angular distributions <3.2 MeV [7], replacing the analysis of Stewart and Horsley [8], which was used up to and including ENDF/B-VI.4. The JENDL-3.3 deuterium data differ from the ENDF/B data with respect to: the elastic scattering cross section (being very slightly lower in the 50 to 500 keV region); the origin of the angular scattering distributions (i.e., nuclear model calculations based on a Faddeev three-body scattering formalism [9]); and, the energy and angular resolution used in the representation of elastic scattering.

The probability distributions for elastic scattering in the centre-of-mass (CM) reference frame are shown as a function of energy and cosine of the scattering angle (μ) for ENDF/B-VII.b1, ENDF/B-VI.4 (using equivalent data from ENDF/V release 2) and JENDL-3.3 in Figs. 1 to 3, respectively, as obtained with the Nuclear and Atomic Data System [10] developed at the

---

[a] MCNP is a trademark of the Regents of the University of California, Los Alamos National Laboratory.

Lawrence Livermore National Laboratory. Tab. 1 lists the specific energies at which data are tabulated and the number of angles (i.e., cosine bins) used. Although the distributions shown are largely based on evaluations using theoretical formalisms, the preference for backward ($\mu<0$) neutron scattering by ^{2}H at energies from 220 keV to about 1.5 MeV had been observed in early measurements [11] and interpreted as a consequence of interference between S waves with negative phase shift and P waves with positive phase shift.

It is noted from Tab. 1 that the energy/angular resolution of the elastic scattering distributions differs significantly among the three data files. In particular, the energy resolution of the distribution for ENDF/B-VII.b1 appears to be relatively coarse between 0.1 and 1.0 MeV.

The difference between the ENDF/B-VI.4 and ENDF/B-VII.b1 energy/angle distributions at energies ≤ 3.2 MeV is shown in Fig. 4, assuming linear interpolation of the respective tabulated values to a uniform energy grid at 0.1 MeV intervals and using 41 cosine values at each energy. Fig. 4 indicates that backscatter ($\mu<0$) is more pronounced in ENDF/B-VI.4, especially at $\mu=-1$.

In addition, a series of modified ENDF/B-VII.b1 and ENDF/B-VI.4 deuterium ACE files was produced in which the angular scattering distributions were forced to have equiprobable cosine bin values from low neutron energy up to a maximum energy that ranged progressively up to 3.2 MeV (up to 9.7 MeV for ENDF/B-VII.b1). In the equiprobable case, each cosine bin is assigned the same probability of 0.5. Calculations with these ACE files were performed only for the cases of an inner sphere of pure ^{235}U or NU metal and a 20-cm ^{2}H reflector thickness.

2.3 MCNP5 Calculations

Each MCNP5 calculation started with a single fission neutron at the centre of the inner sphere. Each case used 1050 cycles of 60,000 neutrons with 50 inactive cycles. The statistical uncertainties in the calculated k_{eff} values are ≤ 0.11 mk (1σ).

3. Results

The MCNP5 k_{eff} values calculated using the various deuterium ACE files and different inner uranium sphere compositions are listed in Tab. 2 as a function of deuterium reflector thickness. In Tab. 2, "^{235}U (NU)" refers to ^{235}U at the nuclide number density corresponding to NU metal and, similarly, "^{238}U (NU)" refers to ^{238}U at the nuclide number density corresponding to NU metal.

The k_{eff} values calculated for the reference ENDF/B-VII.b1 ^{2}H data and a ^{235}U-metal inner sphere increase smoothly from about 0.998 with no ^{2}H reflector to about 1.229 with a 100-cm-thick reflector. Fig. 5 shows the difference in the k_{eff} values with respect to the reference values as a function of the deuterium reflector thickness when different deuterium ACE files are used (solid upper two curves) or when the composition of the inner sphere is varied (dashed lower three curves). The topmost curve in Fig. 5 shows a gain in k_{eff} of up to 10.79 ± 0.15 mk when the ENDF/B-VI.4-based deuterium data are used and the inner sphere is pure ^{235}U. Similarly, the next lower curve shows a peak gain of 9.41 ± 0.15 mk with JENDL-3.3.

Figure 1: ENDF/B-VII.b1 energy/angle scattering distribution for ^{2}H [10].

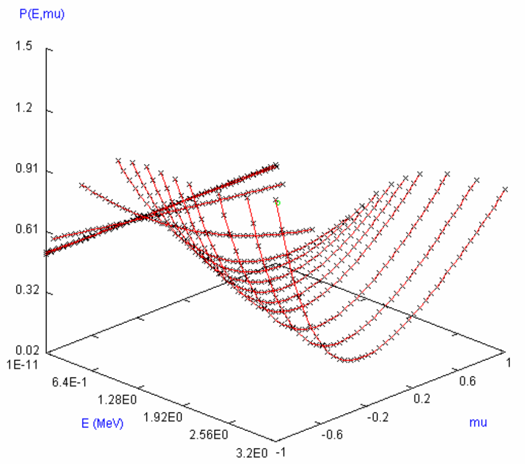

Figure 2: ENDF/B-VI.4 energy/angle scattering distribution for ^{2}H (same as ENDF/B-V.r2 [10])

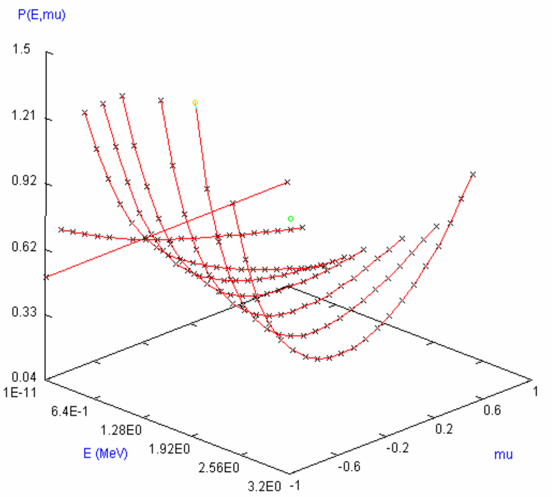

Figure 3: JENDL-3.3 energy/angle scattering distribution for ^{2}H [10].

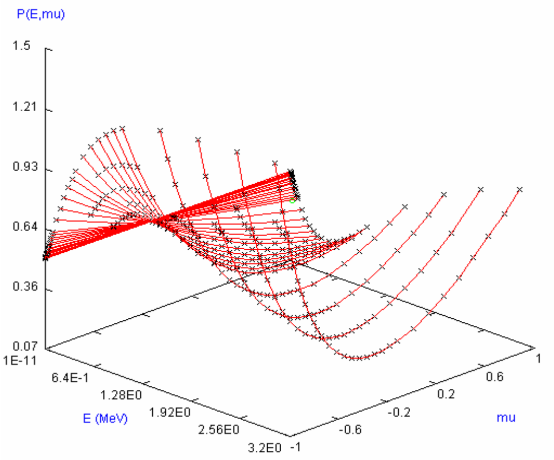

Table 1: Resolution of energy/angle scattering distributions for deuterium.

	ENDF/B-VII.b1		ENDF/B-VI.4		JENDL-3.3	
	Energy (MeV)	# of angles	Energy (MeV)	# of angles	Energy (MeV)	# of angles
1	1.00E-11	2	1.00E-11	2	1.00E-11	3
2	0.0001	41	0.20	21	3.00E-11	3
3	0.001	41	0.50	21	1.00E-10	3
4	0.01	41	0.75	21	3.00E-10	3
5	0.10	41	1.00	21	1.00E-09	3
6	0.50	41	1.50	21	3.00E-09	3
7	1.00	41	1.95	21	1.00E-08	3
8	1.20	41	2.45	21	2.53E-08	3
9	1.40	41	3.27	21	1.00E-07	3
10	1.60	41			3.00E-07	3
11	1.80	41			1.00E-06	3
12	2.00	41			3.00E-06	3
13	2.40	41			1.00E-05	3
14	2.80	41			3.00E-05	3
15	3.20	41			0.0001	3
16					0.0002	3
17					0.0003	3
18					0.0004	3
19					0.0005	3
20					0.0006	3
21					0.0007	3
22					0.0008	3
23					0.0009	3
24					0.0010	3
25					0.0015	3
26					0.0020	3
27					0.0025	3
28					0.0030	3
29					0.0035	3
30					0.004	3
31					0.005	3
32					0.006	3
33					0.007	3
34					0.008	3
35					0.009	3
36					0.010	3
37					0.015	3
38					0.020	3
39					0.025	3
40					0.030	3
41					0.035	3
42					0.04	3
43					0.05	3
44					0.06	3
45					0.07	3
46					0.08	3
47					0.09	3
48					0.10	3
49					0.15	4
50					0.20	5
51					0.25	6
52					0.30	6
53					0.35	7
54					0.40	8
55					0.50	9
56					0.60	9
57					0.70	11
58					0.80	12
59					0.90	12
60					1.00	12
61					1.50	14
62					2.00	14
63					2.50	15
64					3.00	17

Figure 4: Difference between interpolated energy/angle scattering probability distributions: ENDF/B-VI.4 – ENDF/B-VII.b1.

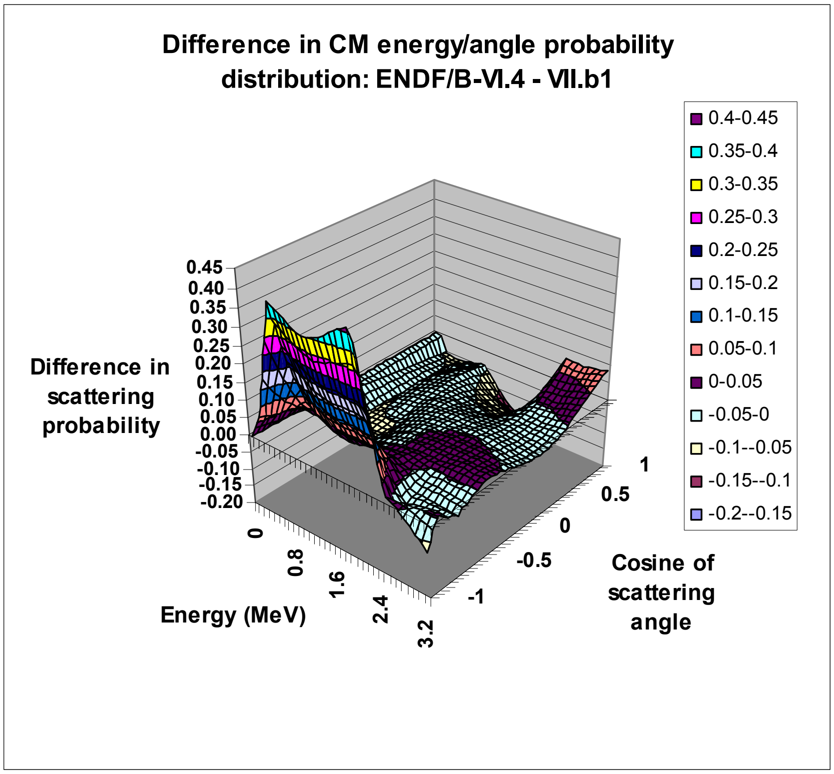

Table 2: MCNP5 k_{eff} values for various ^{2}H ACE files and U compositions.

	^{235}U inner sphere			^{235}U (NU) sphere		NU inner sphere		^{238}U (NU) sphere	
^{2}H thickness (cm)	ENDF/B-VI.4	JENDL-3.3	ENDF/B-VII.b1	ENDF/B-VI.4	ENDF/B-VII.b1	ENDF/B-VI.4	ENDF/B-VII.b1	ENDF/B-VI.4	ENDF/B-VII.b1
0	0.997757 ± 0.000078	0.997757 ± 0.000078	0.997757 ± 0.000078	0.007454 ± 0.000001	0.007454 ± 0.000001	0.185642 ± 0.000030	0.185642 ± 0.000030	0.174147 ± 0.000030	0.174147 ± 0.000030
1	1.026267 ± 0.000078	1.025683 ± 0.000079	1.023606 ± 0.000080	0.008258 ± 0.000001	0.008175 ± 0.000001	0.186520 ± 0.000031	0.186412 ± 0.000030	0.174276 ± 0.000030	0.174295 ± 0.000030
2	1.046544 ± 0.000082	1.045838 ± 0.000082	1.042139 ± 0.000079	0.009150 ± 0.000002	0.008972 ± 0.000002	0.187201 ± 0.000030	0.187089 ± 0.000029	0.174276 ± 0.000030	0.174277 ± 0.000030
5	1.086698 ± 0.000085	1.085538 ± 0.000084	1.079482 ± 0.000088	0.013472 ± 0.000007	0.012897 ± 0.000006	0.189845 ± 0.000028	0.189524 ± 0.000031	0.174292 ± 0.000031	0.174289 ± 0.000029
10	1.124460 ± 0.000091	1.123214 ± 0.000091	1.115120 ± 0.000095	0.030779 ± 0.000021	0.029117 ± 0.000021	0.197774 ± 0.000033	0.197047 ± 0.000031	0.174283 ± 0.000029	0.174320 ± 0.000030
20	1.164909 ± 0.000099	1.163778 ± 0.000096	1.154495 ± 0.000096	0.094844 ± 0.000048	0.091180 ± 0.000048	0.224782 ± 0.000039	0.223332 ± 0.000039	0.174305 ± 0.000030	0.174323 ± 0.000029
100	1.240233 ± 0.000110	1.238854 ± 0.000104	1.229444 ± 0.000109	0.289859 ± 0.000086	0.285678 ± 0.000088	0.313860 ± 0.000056	0.312153 ± 0.000055	0.174265 ± 0.000030	0.174361 ± 0.000029

Figure 5: Sensitivity of MCNP5 Δk_{eff} values to ^{2}H nuclear data files and U composition as a function of ^{2}H reflector thickness.

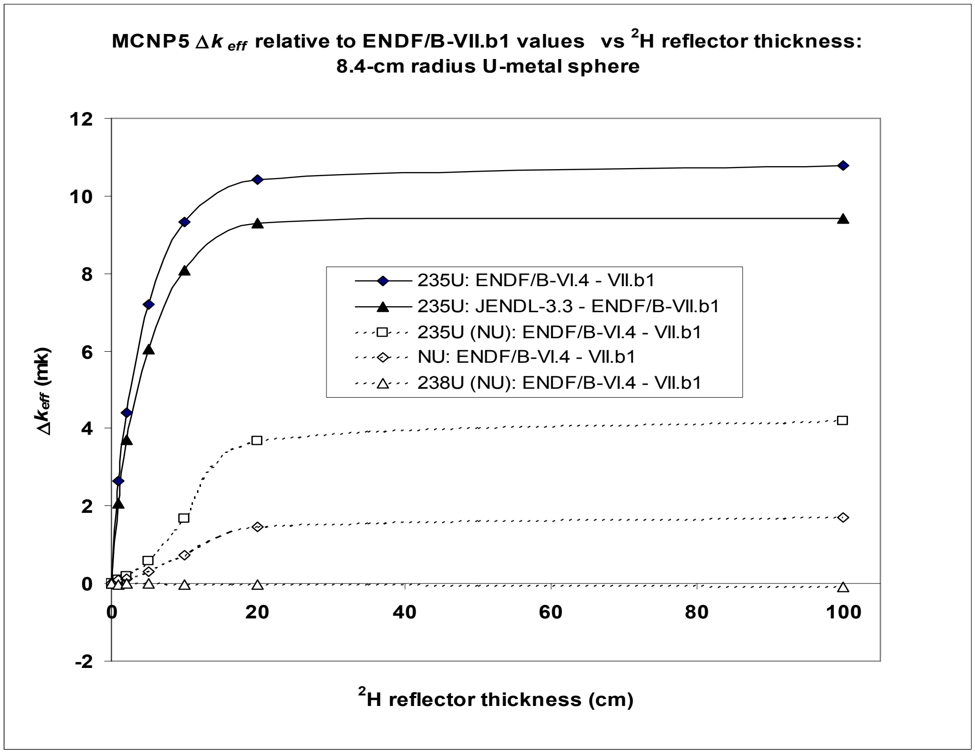

The lowest three curves in Fig. 5 show the Δk_{eff} values obtained when the ENDF/B-VI.4 deuterium data are used and the composition of the uranium metal sphere is: pure ^{235}U at the nuclide number density of ^{235}U in NU metal (maximum $\Delta k_{eff} = 4.18 \pm 0.12$ mk); NU metal (maximum $\Delta k_{eff} = 1.71 \pm 0.08$ mk), and pure ^{238}U at the nuclide number density of ^{238}U in NU metal (maximum $\Delta k_{eff} = -0.10 \pm 0.04$ mk).

The absolute k_{eff} values for these NU-based inner-sphere cases are very low (<0.313) since the radius is kept fixed. It is interesting to note that the lowest keff value is obtained for the bare, low-density ^{235}U sphere (0.00745) as a result of its extreme neutron leakage (99.7%).

The observance of a high Δk_{eff} in the pure ^{235}U metal sphere case and a much lower sensitivity in the NU case is consistent with the behaviour observed in the HST and ZED-2 simulations.

With the exception of the pure ^{238}U inner-sphere case, the Δk_{eff} values in Fig. 5 increase with the amount of deuterium present, i.e., with increasing deuterium reflector thickness and reduced neutron leakage. This behaviour contradicts the observed sensitivities in the HST (high leakage) and ZED-2 (low leakage) simulations and, hence, suggests that total neutron leakage from the system, per se, is not the main distinguishing factor between the two sets of experimental results that affects their k_{eff} sensitivity to the deuterium nuclear data.

Fig. 6 shows the k_{eff} values obtained when the angular scattering distribution for deuterium is altered to have equiprobable cosine bin values up to the neutron energy value indicated on the horizontal axis for the case of an inner sphere of pure ^{235}U metal and a 20-cm-thick ^{2}H reflector. The ENDF/B-VII.b1 k_{eff} values decrease by up to about 29 mk, with most of the loss occurring at energies <2 MeV and both data sets producing similar k_{eff} values above about 1 MeV.

Figure 6: MCNP5 k_{eff} values for ^{235}U-metal inner sphere as a function of the maximum equiprobable cosine bin energy

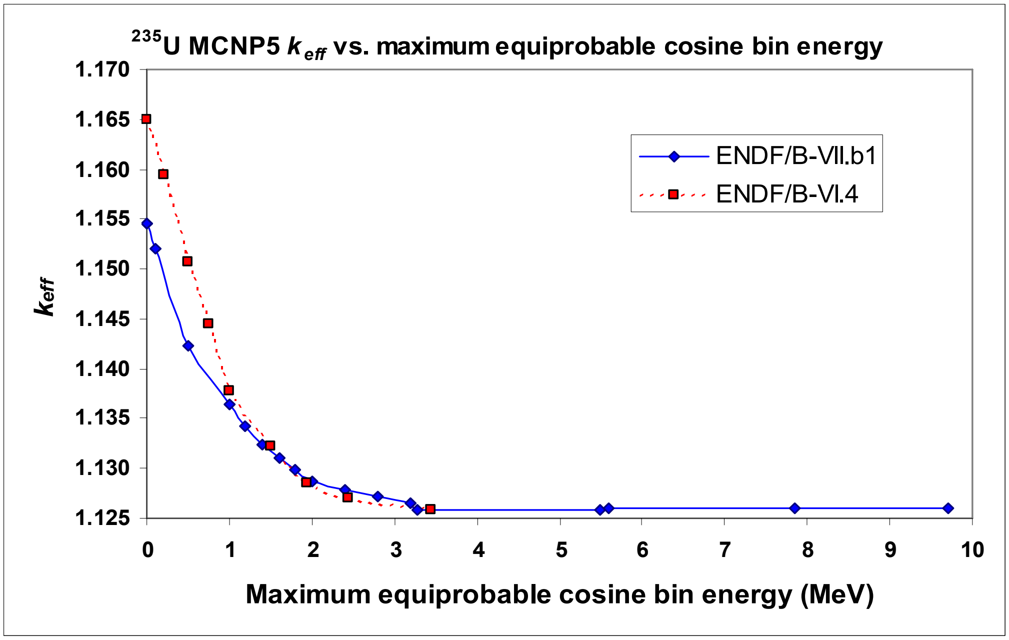

Fig. 7 shows corresponding results for an NU-metal inner sphere over a reduced energy range up to 3.2 MeV. The reference ENDF/B-VII.b1 k_{eff} values indicate reduced sensitivity, decreasing by up to about 4.5 mk. Once again, most of the reactivity loss occurs at energies below 2 MeV and both the ENDF/B-VII.b1 and -VI.4 data produce similar results above about 1 MeV.

Figure 7: MCNP5 k_{eff} values for NU-metal inner sphere as a function of the maximum equiprobable cosine bin energy

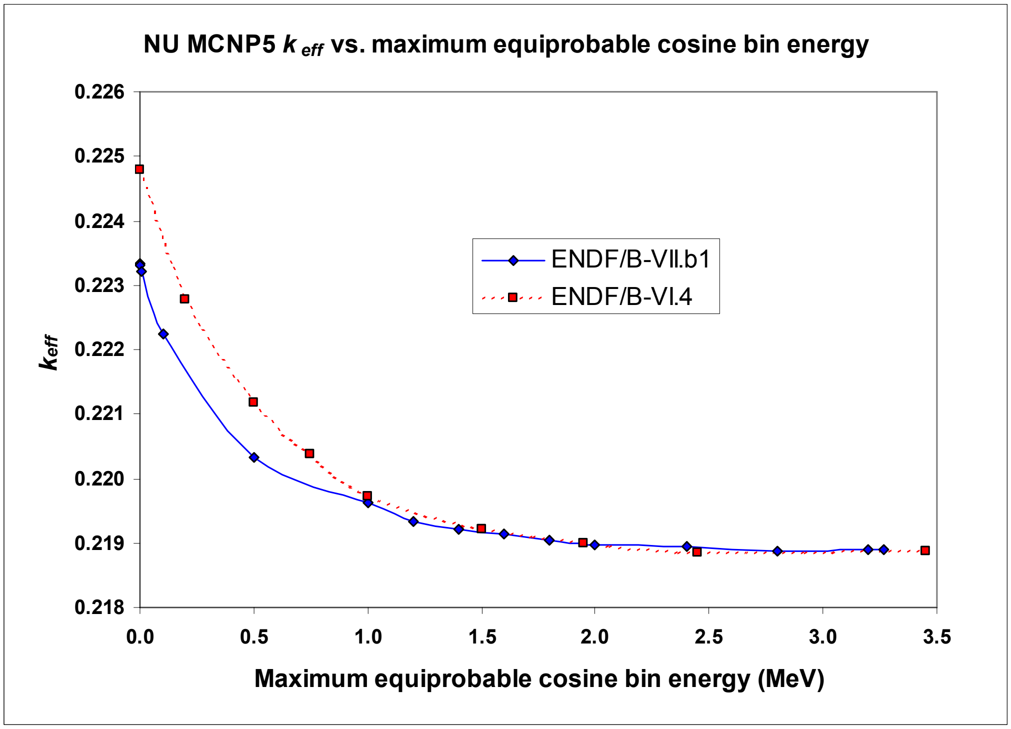

4. Discussion

The fact that higher k_{eff} values are obtained with the ENDF/B-VI.4 and JENDL-3.3 deuterium ACE files for the spherical benchmark model is clearly consistent with the generally higher degree of backscatter that they possess near μ=-1 relative to the reference ENDF/B-VII.b1 values (see Figs. 1 to 4) and is also consistent with corresponding changes in the calculated neutron leakage. Similar Δk_{eff} behaviour is observed in simulations of the HST and ZED-2 critical experiments, with the exception of ZED-2 cases involving D_2O-cooled fuel channels [4].

The Δk_{eff} values obtained for the pure ^{235}U-metal cases are similar to those obtained in calculations for the HST critical experiments when the ^{2}H reflector thickness is ≥ 20 cm, suggesting that the simple spherical model may provide an adequate neutronic surrogate of the HST systems. However, additional, more detailed investigation of other neutronic characteristics, such as reaction rates and flux spectra, and including additional cases with ^{2}H in the inner sphere at various concentrations would be needed to demonstrate this adequacy more convincingly.

The Δk_{eff} values obtained for the NU-metal case and a ^{2}H reflector thickness ≥ 20 cm are within a factor of two of those obtained in ZED-2 simulations [4] and would be reduced further if a larger NU-metal sphere was used with lower neutron leakage. However, a different benchmark model would be needed to serve as a surrogate for ZED-2 cases involving D_2O-cooled fuel channels, which show a small Δk_{eff} (<1 mk) of opposite sign [4]. Nevertheless, some of the observations made here, such as the increase in Δk_{eff} with increasing ^{2}H reflector thickness and decrease with ^{238}U content, suggest that related trends might be found in ZED-2 experiments at different lattice pitches and using fuel rods of different material densities (e.g., U-metal and UO_2) and different fuel-pin radii.

Although the Δk_{eff} values in Fig. 5 appear to be qualitatively consistent with the HST and ZED-2 Δk_{eff} values, quite different behaviour is observed if one plots $\Delta\rho$ values, due to the low k_{eff} values for the NU-based cases. In particular, the ^{235}U (NU) and NU cases then show the highest sensitivity, with an extreme $\Delta\rho$ value of 3309 mk for the former at a 5-cm reflector thickness.

While the reactivity sensitivity studies performed here are empirical, more systematic investigations of the sensitivity to the deuterium data could be performed using appropriate tools, such as the SCALE (Standardized Computer Analyses for Licensing Evaluation) / TSUNAMI (Tools for Sensitivity and Uncertainty Analysis Methodology Implementation) [12] code system developed at the Oak Ridge National Laboratory (ORNL). However, while the TSUNAMI code can assess the sensitivity to the ^{2}H elastic scattering cross section, it does not currently consider the details of the angular distributions.

5. Conclusion

The MCNP5 k_{eff} results for a simplified spherical benchmark model show a large sensitivity to the deuterium data files, up to 10.8 mk, when the inner sphere is pure ^{235}U and only about 1.7 mk when it is NU, indicating that uranium enrichment is a key factor in the different sensitivities observed for the HST and ZED-2 critical measurements. Further, it appears that the presence of ^{238}U in NU reduces a significant sensitivity (up to 4.2 mk) that would otherwise be apparent due to ^{235}U at the reduced nuclide number density of NU metal. The importance of accurate angular scattering distributions for deuterium, especially at energies <2 MeV, was demonstrated using calculations with angular distributions modified to have equiprobable cosine bin values up to a given energy. Moreover, the k_{eff} results obtained using the modified ENDF/B-VII.b1 and -VI.4 deuterium ACE files differ significantly only at energies <1 MeV, suggesting that this energy range be given priority should new scattering distribution measurements be undertaken.

Acknowledgements

The author wishes to thank R. Zajac, then at the National Nuclear Data Center, Brookhaven National Laboratory, and R.D. Mosteller of LANL for providing the ENDF/B-VII.b1 and -VI.4 ACE files, respectively, used in this work.

References

1) R.D. Mosteller and R.C. Little, ENDF/B-VI and Preliminary ENDF/B-VII Results for the MCNP Criticality Validation Suite, LA-UR- 04-7356 , 2004 Annual Meeting of the Cross Section Evaluation Working Group, Brookhaven National Laboratory, November 2 - 4, 2004, http://www.nndc.bnl.gov/proceedings/2004csewgusndp/wednesday/ENDFBVIIeval_valid/04_Mosteller.pdf.
2) R.D. Mosteller, J.M. Campbell and R.C. Little, Reactivity Impact of ENDF/B-VI Cross Sections for Deuterium in Heavy-Water Solution Benchmarks, LA- UR- 05-0330, 2005 Annual Meeting of the American Nuclear Society, June 5 - 9, 2005, San Diego, CA.
3) International Handbook of Evaluated Criticality Safety Benchmark Experiments, NEA/NSC/DOC(95)03, OECD Nuclear Energy Agency (2005 Edition).
4) R.D. Mosteller, K.S. Kozier, J.M. Campbell and R.C. Little, "Reactivity Impact of Deuterium Cross Sections for Heavy-Water Benchmarks," LA-UR-05-0787, proceedings of the International Topical Meeting on Mathematics and Computation, Supercomputing, Reactor Physics, and Nuclear and Biological Applications, Avignon, France, September 12-15, 2005.
5) X-5 Monte Carlo Team, "MCNP — A General Monte Carlo N-Particle Transport Code, Version 5," Los Alamos National Laboratory report LA-UR-03-1987 (April 2003).
6) K. Kosako, N. Yamano, T. Fukahori, K. Shibata and A. Hasegawa, "The Libraries FSXLIB and MATXSLIB based on JENDL-3.3," JAERI-Data/Code 2003-011 (July 2003).
7) P. G. Young, G. M. Hale, and M.B. Chadwick, Evaluation of n + ^{2}H Cross Sections for the Energy Range 1.0E-11 to 150 MeV, http://t2.lanl.gov/publications/la150/n2h.pdf (1997).
8) A. Horsley and L. Stewart, Evaluated Neutron Cross Sections for Deuterium, LA-3271, http://www.fas.org/sgp/othergov/doe/lanl/lib-www/la-pubs/00420216.pdf (1968).
9) W. Ebenhoh, Nucl. Phys. A, 191, pp. 97 (1972).
10) Nuclear and Atomic Data System, LLNL, http://nuclear.llnl.gov/CNP/nads/NADSApplet.html..
11) R.K. Adair, A. Okazaki and M. Walt, "Scattering of Neutrons by Deuterons," Phys. Rev., Vol. 89, pp. 1165 (1953).
12) TSUNAMI, Tools for Sensitivity and Uncertainty Analysis Methodology Implementation, ORNL, http://www.ornl.gov/sci/scale/tsunami/.